The anisotropy of optical conductivity derived from the energy splitting in iron arsenides

Journal of Physics: Conference Series **400** (2012) 022113 doi:10.1088/1742-6596/400/2/022113

The anisotropy of optical conductivity derived from the energy splitting in iron arsenides

K Sugimoto[1], E Kaneshita[2] and T Tohyama[1,3]

[1]Yukawa Institute for Theoretical Physics, Kyoto University, Kyoto 606-8502, Japan
[2]Sendai National College of Technology, Sendai 989-3128, Japan
[3]JST, Transformative Research-Project on Iron Pnictides (TRIP), Chiyoda, Tokyo 102-0075, Japan

E-mail: koudai@yukawa.kyoto-u.ac.jp

Abstract. We examine the anisotropy of optical conductivity above the Néel temperature in iron arsenides by mean-field calculation in a five-band Hubbard model. In order to represent the anisotropy, we artificially introduce the energy splitting between d_{zx} and d_{yz}. The calculated spectra are not enough to explain the anisotropy observed in experiments. The optical conductivity in the low-energy region is consistent with the observation, while in the high-energy region not. This implies that there should be some other effects to give rise to the anisotropy in the high-energy region.

1. Introduction

In-plane anisotropy is remarkable in iron arsenide superconductors and their parent compounds. In the antiferromagnetically ordered phase with orthorhombic structure, an electric anisotropy in the FeAs plane has been reported from scanning tunnelling microscopy [1], resistivity [2, 3], optical conductivity [4, 5], and angle resolved photoemission spectroscopy (ARPES) [6, 7]. The ARPES measurements above the Néel temperature T_N have shown the lift of degeneracy between d_{zx} and d_{yz} orbitals [8], which indicates a strong influence of the orbital degree of freedom on the nematic order and the electronic anisotropy below T_N [9]. In fact, the in-plane anisotropy of optical conductivity below T_N has been explained by taking into account orbital characters of interband excitation [10, 11].

In this paper, we discuss the anisotropic behavior of optical conductivity above T_N with an energy splitting of d_{zx} and d_{yz} orbitals. Experiments [4, 12] show an anisotropy above T_N, and we compare them with our result. We find that the energy splitting is not enough to explain the anisotropy of optical conductivity in a wide range of energy.

2. Model and method

Considering an Fe square lattice, we start with the mean-field Hamiltonian for a d-electron system

$$H_{\rm MF} = \sum_{\mu,\nu} \sum_{\boldsymbol{k},\sigma} H_{\mu,\nu}(\boldsymbol{k},\sigma) c^{\dagger}_{\boldsymbol{k}\mu\sigma} c_{\boldsymbol{k}\nu\sigma}, \tag{1}$$

where $c^{\dagger}_{\boldsymbol{k}\mu\sigma}$ creates an electron with a wave vector $\boldsymbol{k}$ and a spin σ at an orbital μ. The component of $H_{\rm MF}$ is

$$\begin{aligned} H_{\mu,\nu}(\boldsymbol{k},\sigma) = &\sum_{\boldsymbol{\Delta}} t(\Delta_x,\Delta_y;\mu,\nu)e^{i\boldsymbol{k}\cdot\boldsymbol{\Delta}} + \epsilon_\mu\delta_{\mu,\nu} \\ &+ J\Big[\big(-\sum_{\mu'}\langle n_{\mu'\mu'\sigma}\rangle + 5\langle n_{\mu\mu\sigma}\rangle - 2n_0\big)\delta_{\mu,\nu} + \big(4\langle n_{\nu\mu\sigma}\rangle + \langle n_{\mu\nu\sigma}\rangle\big)(1-\delta_{\mu,\nu})\Big] \\ &+ U\Big[\big(n_0 - \langle n_{\mu\mu\sigma}\rangle^*\big)\delta_{\mu,\nu} - \langle n_{\mu\nu\sigma}\rangle^*(1-\delta_{\mu,\nu})\Big], \end{aligned} \tag{2}$$

where U is the intraorbital Coulomb interaction, J is the Hund coupling and the pair hopping, $\langle n_{\mu\nu\sigma}\rangle \equiv N^{-1}\sum_{\boldsymbol{k}}\langle c^{\dagger}_{\boldsymbol{k}\mu\sigma}c_{\boldsymbol{k}\nu\sigma}\rangle$, and $n_0 \equiv \sum_{\mu,\sigma}\langle n_{\mu\mu\sigma}\rangle$ (in $BaFe_2As_2$, $n_0 = 6$). N is the number of $\boldsymbol{k}$ points in the first Brillouin zone (BZ). $t(\Delta_x,\Delta_y;\mu,\nu)$ and ϵ_μ are the in-plain hopping integrals and on-site energies, respectively, presented by Ref. [13]. The Fe-Fe bond length is set to unity and the x- and y-directions are along to the nearest Fe-Fe bonds.

We self-consistently solve mean-field equations with $\langle n_{\mu\nu\sigma}\rangle$. The quasiparticle state $\gamma^{\dagger}_{\boldsymbol{k}\epsilon\sigma} = \sum_\mu \psi_{\mu\epsilon\sigma}(\boldsymbol{k})c^{\dagger}_{\boldsymbol{k}\mu\sigma}$ diagonalizes the Hamiltonian with the eigenvalue $E_{\boldsymbol{k}\epsilon\sigma}$, where ϵ is the band index. The average $\langle\cdots\rangle$ is taken at zero temperature in our calculation. The computations are performed on a system with $N = 500\times500$. We set $U = 1.2$ eV and $J = 0.23$ eV as our previous calculation [11]. Comparing the results with those in the case $U, J = 0$, we find that the results are almost insensitive.

Interband contributions to the real part of the optical conductivity are expressed as [15]

$$\sigma_{\alpha\beta}(\omega>0) = \frac{-\pi}{N\omega}\Big(\frac{e}{\hbar}\Big)^2 \sum_{\boldsymbol{k},\epsilon,\epsilon',\sigma}[f(E_{\boldsymbol{k}\epsilon\sigma}) - f(E_{\boldsymbol{k}\epsilon'\sigma})]\zeta^{(\alpha)}_{\boldsymbol{k}\epsilon\epsilon'\sigma}[\zeta^{(\beta)}_{\boldsymbol{k}\epsilon\epsilon'\sigma}]^*\delta(E_{\boldsymbol{k}\epsilon\sigma} - E_{\boldsymbol{k}\epsilon'\sigma} - \omega), \tag{3}$$

where e is the elementary charge, f is the Fermi distribution function, and $\zeta^{(\alpha)}_{\boldsymbol{k}\epsilon\epsilon'\sigma}$ arising from the current operator has the form

$$\zeta^{(\alpha)}_{\boldsymbol{k}\epsilon\epsilon'\sigma} = \sum_{\boldsymbol{\Delta},\mu,\nu}\Delta^{(\alpha)}t(\Delta_x,\Delta_y;\mu,\nu)e^{-i\boldsymbol{k}\cdot\boldsymbol{\Delta}}\psi_{\mu\epsilon\sigma}(\boldsymbol{k})\psi^*_{\nu\epsilon'\sigma}(\boldsymbol{k}), \tag{4}$$

with $\Delta^{(\alpha)}$ the α component of the vector $\boldsymbol{\Delta}$. Equation (3) does not contain the Drude component coming from the intraband transition.

We use a renormalized energy scale with a factor 1/3 to the energy axis: 0.1 eV in the figures of optical conductivity shown below corresponds to 0.3 eV on the original scale of our calculations. This factor is taken from comparisons between the dispersion observed by ARPES and the theoretical dispersion determined by first-principles calculation [14, 16]. The factor corresponds to the band renormalization effect that is not included in either the first-principles calculation or our mean-field calculation.

3. Optical conductivity

As discussed above, the electric anisotropy has been confirmed by recent experiments above the magneto-structural transition, and this suggests the presence of nematic order. From the comparison between ARPES and band structure calculation [8], this effect would be explained by on-site energy splitting δ between d_{zx} and d_{yz}. We replace the on-site energies ϵ_{zx} and ϵ_{yz} in Equation (2) with

$$\epsilon'_{zx} = \epsilon_{zx} + \frac{\delta}{2}, \quad \epsilon'_{yz} = \epsilon_{yz} - \frac{\delta}{2}. \tag{5}$$

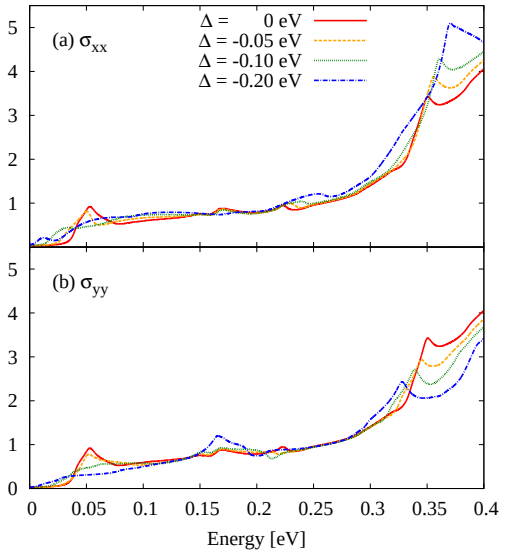

Figure 1. The evolution of optical conductivity by the energy splitting δ between d_{zx} and d_{yz} orbitals along the x-direction in (a) and along the y-direction in (b). The Drude component is not included. The optical conductivity is normalized by $(\frac{e}{2\hbar})^2$.

Since the d_{zx} and d_{yz} band rises up and falls down, respectively, in the ARPES measurement, δ should be negative.

The evolution of optical conductivity $\sigma_{xx}(\omega)$ and $\sigma_{yy}(\omega)$ along the x- and y-direction is illustrated in Figure 1 (a) and (b), respectively. When $\delta = 0$, these completely coincide. Corresponding to the appearance of the energy splitting, σ_{xx} and σ_{yy} show different behavior. In Figure 1 (a), σ_{xx} is suppressed around 0.05 eV and enhanced around 0.1 eV and 0.37 eV. In Figure 1 (b), σ_{yy} is also suppressed around 0.05 eV and, in contrast to σ_{xx}, suppressed around 0.37 eV. In addition to these changes, a peak structure appears around 0.17 eV in σ_{yy}.

We examine the excitations at 0.1 eV, where σ_{xx} is enhanced while σ_{yy} is almost unchanged by the energy splitting. The excitations contributing to σ_{xx} and σ_{yy} occur near the X point in the BZ. In the $\boldsymbol{k}$ points where the large contribution to σ_{xx} with the energy splitting, the orbitals of the initial and final states are mainly d_{xy} and d_{yz}, respectively. However, in the same $\boldsymbol{k}$ points with no energy splitting, the orbitals of the initial and final states are mixture of d_{yz} and d_{xy}. On the other hand, the excitations contributing to σ_{yy} occur on the k_x axis; the orbitals of the initial and final states are dominantly d_{yz} and d_{xy}, respectively, in either case of the finite or zero energy splitting. Thus, the change of orbital character induces the anisotropy of optical conductivity.

In order to compare σ_{xx} with σ_{yy}, the optical conductivity of each direction at $\delta = -0.20$ eV is plotted together in Figure 2. This shows that σ_{xx} is larger than σ_{yy} in the whole energy range, except for around 0.17 eV, where a peak structure appears in σ_{yy}. In the optical conductivity measurement above T_N [12], σ_{xx} is more suppressed than σ_{yy} in low-energy region (below 1350 cm^{-1}), while σ_{yy} is slightly larger than σ_{xx} in the higher-energy region. Our results are, therefore, consistent with the measurement in the low-energy region, but are not in high-energy region.

4. Conclusion

We introduce the on-site energy splitting between d_{zx} and d_{yz} and obtain that the anisotropy of optical conductivity above T_N is consistent with the measurement in the low-energy region. However, the anisotropy in the high-energy region is inconsistent with the measurement. This implies that we should consider another effect to cause energy-dependent anisotropy, such as energy dependence of self-energy.

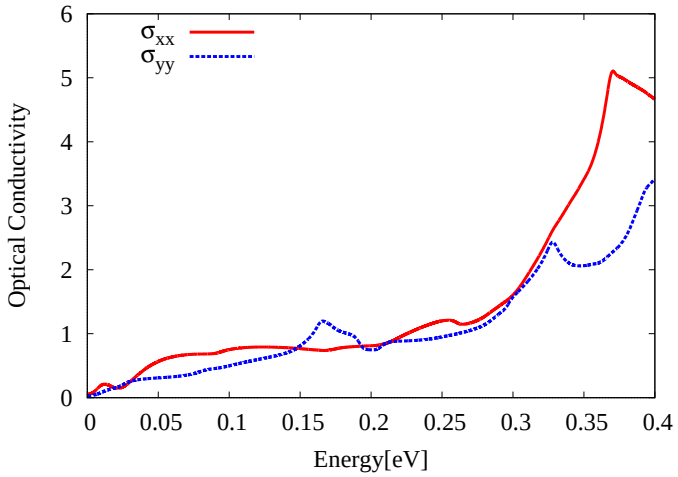

Figure 2. The comparison of optical conductivity between $\sigma_{xx}(\omega)$ and $\sigma_{yy}(\omega)$ where the energy-splitting $\delta = -0.20$ eV.

After compiling this work, we became aware of a similar calculation about the anisotropy of optical conductivity under orbital nematic order [17].

Acknowledgments
We would like to thank M. Nakajima for stimulating discussions and for providing us their data prior to publication. This work was supported by a Grant-in-Aid for Scientific Research from the Ministry of Education, Culture, Sports, Science and Technology of Japan; the Global COE Program "The Next Generation of Physics, Spun from University and Emergence"; the Next Generation Supercomputing Project of Nanoscience Program; and Yukawa Institutional Program for Quark-Hadron Science. The numerical computation in this work was carried out at the Yukawa Institute Computer Facility.

References
[1] Chuang T-M, Allan M P, Lee J, Xie Y, Ni N, Bud 'ko S L, Boebinger G S, Canfield P C and Davis J C 2010 Science **327** 181
[2] Tanatar M A *et al* ,2010 Phys. Rev. B **81** 184508
[3] Chu J-H, Analytis J G, De Greve K, McMahon P L, Islam Z, Yamamoto Y and Fisher I R 2010 Science **329** 824
[4] Dusza A, Lucarelli A, Pfuner F, Chu J-H, Fisher I R and Degiorgi L 2011 EPL **93** 37002
[5] Nakajima M *et al* 2011 J. Phys. Chem. Solids **72** 511
[6] Kim Y *et al* 2011 Phys. Rev. B **83** 064509
[7] Wang Q *et al* arXiv:1009.0271
[8] Yi M *et al* 2011 Proc. Nat. Acad. Sci. **108** 6878
[9] Chen C-C *et al* 2010 Phys. Rev. B **82** 100504
[10] Yin Z P, Haule K and Kotliar G 2011 Nat. Phys. **7** 294
[11] Sugimoto K, Kaneshita E and Tohyama T 2011 J. Phys. Soc. Jpn. **80** 033706
[12] Nakajima M *et al* arXiv:1106.4967
[13] Kuroki K, Onari S, Arita R, Usui H, Tanaka Y, Kontani H and Aoki H 2008 Phys. Rev. Lett. **101** 087004
[14] Yi M *et al* 2009 Phys. Rev. B **80** 174510
[15] Kaneshita E, Morinari T and Tohyama T 2009 Phys. Rev. Lett. **103** 247202
[16] Yoshida T *et al* 2011 J. Phys. Chem. Solids **72** 465
[17] Lv W and Phillips P arXiv:1105.4630